Molecular Therapy
Nucleic Acids
Original Article

Plasmid encoding microRNA-200c ameliorates periodontitis and systemic inflammation in obese mice

Tadkamol Krongbaramee,[1] Min Zhu,[1] Qingwen Qian,[2] Zeyuan Zhang,[2] Steven Eliason,[3] Yi Shu,[1] Fang Qian,[1] Adil Akkouch,[1] Dan Su,[3] Brad A. Amendt,[1,3,4] Ling Yang,[2] and Liu Hong[1,4]

[1]Iowa Institute for Oral Health Research, College of Dentistry, the University of Iowa, Iowa City, IA, USA; [2]Department of Anatomy and Cell Biology, Fraternal Order of Eagles Diabetes Research Center, Pappajohn Biomedical Institute, University of Iowa Carver College of Medicine, Iowa City, IA, USA; [3]Department of Anatomy and Cell Biology, Carver College of Medicine, the University of Iowa, Iowa City, IA, USA; [4]Center for Craniofacial Anomalies Research, Carver College of Medicine, the University of Iowa, Iowa City, IA, USA

The present study was conducted to characterize microRNA-200c (miR-200c) and its regulators in adipogenic differentiation, obesity, and periodontitis in obese subjects (PiOSs), and to determine the therapeutic efficacy of plasmid DNA encoding miR-200c as a treatment for PiOSs. We report that highly expressed miR-200c in gingival tissues was downregulated in diet-induced obese (DIO) mice and during adipogenic differentiation of human bone marrow mesenchymal stromal cells (hBMSCs). Local injection of *Porphyromonas gingivalis* lipopolysaccharide (Pg-LPS) in the maxilla interdental gingiva of DIO mice reduced miR-200c in gingival and adipose tissues and induced periodontal inflammation associated with systemic elevation of interleukin-6 (IL-6) and impaired glucose tolerance. The inhibitory functions of Pg-LPS and IL-6 on miR-200c and their effectiveness on Zeb1 were confirmed *in vitro*. Injection of naked plasmid DNA encoding miR-200c into the gingiva effectively rescued miR-200c downregulation, prevented periodontal and systemic inflammation, and alleviated the impaired glucose metabolism in obese mice with LPS-induced periodontitis. Increased circulating exosomal miR-200c and its function on suppressing proinflammatory cytokines and adipogenesis explained the mechanism(s) of gingival application of miR-200c in attenuating systemic inflammation in PiOSs. These results demonstrated that miR-200c reduced by Pg-LPS and IL-6 in periodontitis and obesity might lead to the pathogenesis of PiOSs, and upregulation of miR-200c in the gingiva presents a therapeutic approach for PiOSs.

INTRODUCTION

Periodontitis, a set of inflammatory diseases affecting the tissues surrounding the teeth, is linked to or considered a high-risk factor for rheumatoid arthritis, cognitive impairment, cardiovascular diseases, cancer, obesity, and diabetes.[1–6] The sustained chronic inflammatory state of obesity strongly intersects with periodontitis in the context of both pathogenesis and prognosis.[7–10] Adults with obesity nearly double the prevalence rate of periodontitis compared to non-obese subjects, and periodontitis in obese subjects (PiOSs) results in more severe alveolar bone (AB) loss.[8,11] Obesity has been demonstrated to negatively impact periodontitis in various pathogenic aspects. Specifically, obese individuals have multiple upregulated proinflammatory molecules and processes implicated in periodontitis, including cytokines, chemokines, and T cell function.[12,13] The proinflammatory environment and altered periodontal microbial composition in predisposed obese individuals increases gingival inflammatory responses and periodontal tissue destruction. Increased risk of insulin resistance in obesity also significantly promotes advanced glycation end products at the gingiva, which contributes to more significant periodontal bone loss.[14] Obesity directly diminishes the effectiveness of periodontal therapy and results in inferior outcomes of non-surgical treatment,[15,16] whereas dietary weight loss intervention effectively promotes a reduction in systemic inflammation and improves the outcome of periodontal treatment. Conversely, periodontitis also contributes to elevated systemic inflammatory responses in obesity. Intensive periodontal therapy has been demonstrated to effectively reduce c-reactive protein levels, interleukin-6 (IL-6), and low-density lipoprotein cholesterol in obese patients.[17] Although the imbalance and dysregulation of proinflammatory cytokines, transcription factors, and bone metabolism mediators govern the pathogenic progression of the periodontitis, the underlying molecular mechanisms of a higher prevalence of periodontitis and periodontal tissue destruction in PiOSs still remain unknown. Importantly, surgical treatment is currently required for moderate to advanced periodontitis; unfortunately, the success rate is merely 50%.[18] Therefore, an understanding of the pathogenic mechanism(s) underlying complications between obesity and periodontitis and the development of an efficient and safe therapy against advanced periodontitis in PiOSs are demanded.

Received 12 October 2020; accepted 28 January 2021;
https://doi.org/10.1016/j.omtn.2021.01.030.

Correspondence: Liu Hong, MD, PhD, Iowa Institute for Oral Health Research, College of Dentistry, the University of Iowa, Iowa City, IA, USA.
E-mail: liu-hong@uiowa.edu

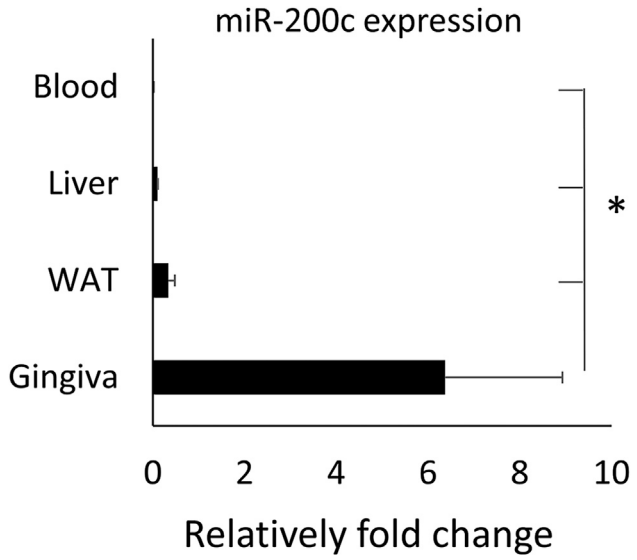

Figure 1. Relative fold changes of *miR-200c* expression in different tissues and organs of 22-week-old C57BL/6J mice

*$p < 0.05$, n = 3.

MicroRNAs (miRNAs or miRs) are small non-coding RNAs that promote the degradation and/or repress the translation of mRNA through sequence-specific interactions with specific mRNA targets. miRNAs have been demonstrated to actively participate in the progression and management of the inflammatory response, including those involved in the onset and development of obesity and periodontitis. Specifically, miRNAs are significantly differentially expressed between a healthy state and periodontitis.[19,20] miRNAs actively regulate adipogenesis and play essential roles in obesity and obesity-associated metabolic diseases.[21] A recent study discovered that miRNAs were differentially expressed in individuals with periodontitis alone, obesity alone, and in PiOSs when compared to healthy controls.[22] Also, miRNAs have emerged as critical transcriptional regulators that target inflammation-related mediators, including tumor necrosis factor alpha (TNF-α), IL-1β, IL-6, and IL-8.[22–25] Thus, manipulating specific miRNAs that participate in the molecular pathogenesis of PiOSs may potentially be developed as a novel and efficient therapeutic tool for PiOSs.

miR-200c is a member of the *miR-200* family that plays an essential role in tumor suppression by inhibiting the epithelial-mesenchymal transition (EMT). *miR-200c* has strong suppressive effects on cell transformation, cancer cell proliferation, migration, invasion, tumor growth, and metastasis.[26–28] While the influence of obesity and PiOSs on *miR-200c* expression in the human gingiva remains unknown, *miR-200c* is significantly reduced in the gingival tissues of periodontitis patients.[29] *Porphyromonas gingivalis* lipopolysaccharide (Pg-LPS) was reported to suppress *miR-200c* in human primary macrophages.[30] Pg also downregulated *miR-200c* by upregulating Zeb1 in gingival epithelial cells.[31] Additionally, *miR-200c* was downregulated in the circulation of obese patients with insulin resistance.[32] *miR-200c* was reported to have a strong association with whole-body insulin sensitivity but was inversely associated with insulin resistance and basal glucose. In animal studies, Chartoumpekis et al.[33] reported that diet-induced obesity (DIO) in mice significantly downregulated *miR-200c* in adipose tissue. Additionally, *miR-200c* has demonstrated strong anti-inflammatory capabilities. Specifically, *miR-200c* attenuated LPS-induced early pulmonary fibrosis and inhibited IL-33 in bronchial asthma.[34,35] *miR-200c* modulated cancer inflammation by reducing nuclear factor κB (NF-κB) activation through Toll-like receptor 4 (TLR-4) and myeloid differentiation primary response 88 (MyD88)-dependent pathways.[36] *miR-200c* reduced IL-8 expression by targeting the inhibitor of NF-κB kinase subunit beta (IKBKB) in the NF-κB signal pathway in breast cancer.[37] Our previous studies have demonstrated that *miR-200c* directly targets 3′ UTRs of IL-6, IL-8, interferon-related developmental regulator 1 (Ifrd1), and chemokine (C-C motif) ligand 5 (CCL-5), and downregulates these proinflammatory and osteoclastogenic mediators in human periodontal ligament, gingival fibroblasts, and the periodontium of periodontitis rats.[38] We have also demonstrated the capabilities of *miR-200c* on upregulating Wnt activity and inhibiting noggin (a novel inducer in adipogenesis) for osteogenic differentiation and bone regeneration.[39,40]

In the present study, we characterized *miR-200c* and its regulators in adipogenic differentiation, obesity, and PiOSs using human cells and mouse models and attempted to explore *miR-200c* as a therapeutic tool for PiOSs. We revealed the downregulation of *miR-200c* in DIO mice and adipogenic differentiated human bone marrow mesenchymal stromal cells (hBMSCs) *in vitro*. Injection of Pg-LPS into the gingiva of DIO mice effectively mimicked the clinical characteristics of PiOSs, including periodontal inflammation associated with systemic elevation of IL-6 and impaired glucose tolerance. Local injection of naked plasmid DNA encoding *miR-200c* in gingival tissues effectively rescued *miR-200c* expression, protected against periodontal and systemic inflammation, and alleviated the impaired glucose metabolism in PiOS mice. Injection of *miR-200c* effectively increased circulating exosomal *miR-200c*, probably explaining the mechanism(s) of gingival application of *miR-200c* in attenuating systemic and white adipose tissue (WAT) inflammation in PiOSs. The monoclonal antibody (mAb) of IL-6 can counteract the function of Pg-LPS on *miR-200c* and Zeb1. These data strongly indicate that the reduction of *miR-200c* induced by Pg-LPS and IL-6 in PiOSs might lead to an imbalance of proinflammatory cytokines and exacerbate inflammatory responses, and upregulating *miR-200c* expression in gingiva would serve as a potential therapeutic approach for PiOSs.

RESULTS

miR-200c is highly expressed in oral gingiva

Figure 1 summarizes the tissue-specific distribution of *miR-200c* in mice. We observed that *miR-200c* was significantly higher expressed in oral gingival tissues than in the liver, WAT, and blood serum. The expression of *miR-200c* in WAT was higher than in the liver and blood serum. No difference between blood and liver was observed.

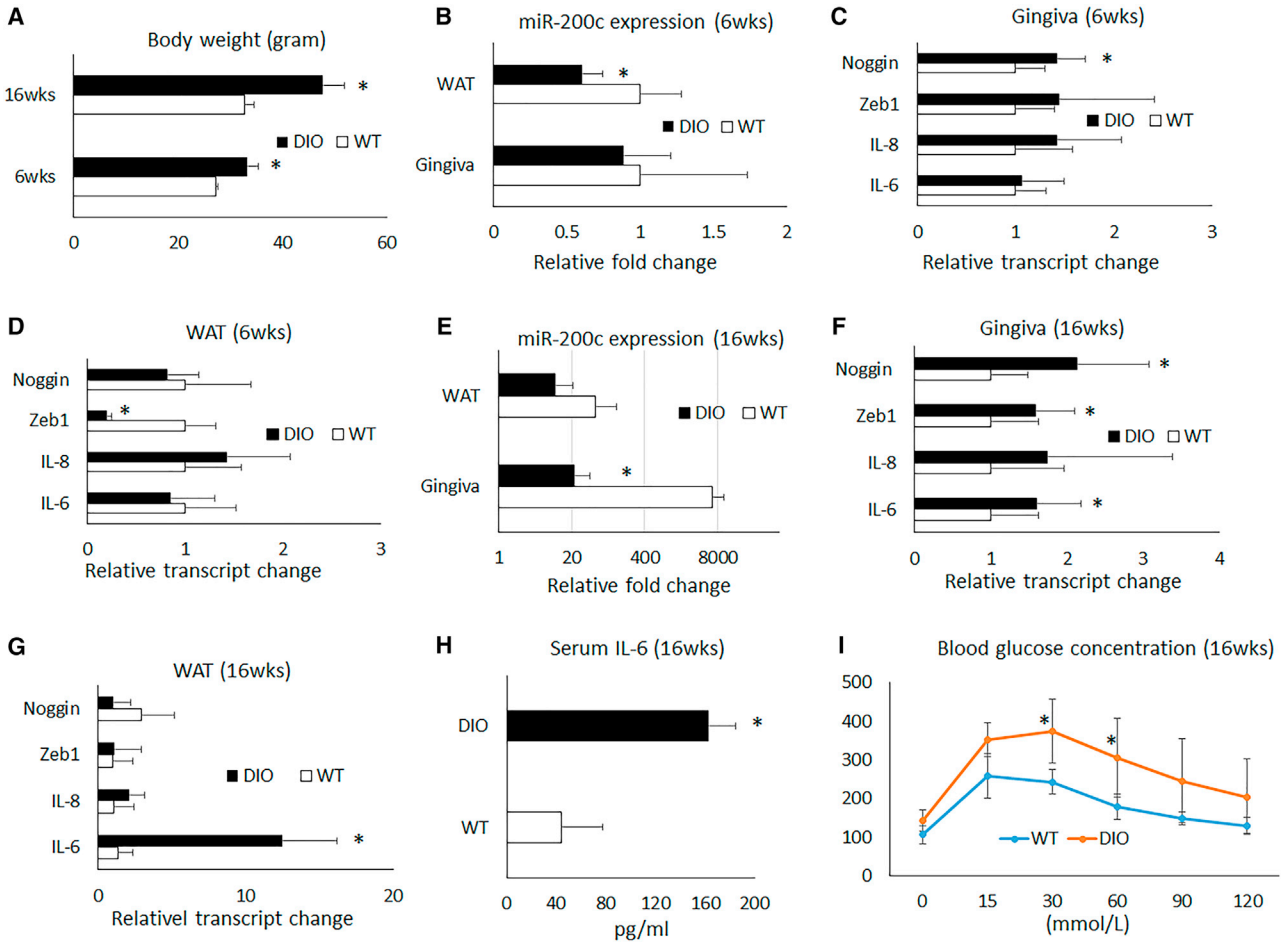

Figure 2. Characteristics of DIO mice fed with an HFD after 6 and 16 weeks

(A) Body weights of mice fed with an HFD for 6 and 16 weeks. (B) Relative fold changes of *miR-200c* in gingiva and WAT in mice fed with an HFD for 6 weeks. (C and D) Relative transcript level changes of noggin, Zeb1, IL-6, and IL-8 in gingival tissues and WAT in mice fed with an HFD for 6 weeks. (E) Relative fold changes of *miR-200c* in gingiva and WAT in mice fed with an HFD for 16 weeks. (F and G) Relative transcript change of noggin, Zeb1, IL-6, and IL-8 in gingival tissues and WAT in mice fed with an HFD for 16 weeks. (H) Concentrations of IL-6 in blood serum in mice fed with an HFD for 16 weeks. (I) Blood glucose concentrations of a GTT test in mice fed with an HFD for 16 weeks. *$p < 0.05$ versus wild-type (WT), n = 3–9.

Obesity downregulated miR-200c and increased proinflammatory cytokines and insulin resistance in mice

For mice, after 6 and 16 weeks, a high-fat diet (HFD) resulted in a significant increase in body weight over a regular diet (RD; Figure 2A). After 6 weeks on an HFD, a significant reduction of *miR-200c* was observed in WAT, while no statistically significant downregulation of *miR-200c* was observed in gingival tissue due to variability. Additionally, 6 weeks of an HFD did not statistically increase *IL-6* and *IL-8*, while noggin was upregulated significantly in gingival tissues. Interestingly, *Zeb1* was downregulated in WAT. However, after 16 weeks on an HFD, we found that *miR-200c* was significantly downregulated in the gingiva of DIO mice (Figure 2E), and transcripts of *IL-6* increased in both gingiva and WAT (Figures 2F and 2G), while IL-8 was hardly changed. Both noggin and *Zeb1* were significantly increased in gingival tissues. Additionally, after 16 weeks on an HFD, the protein level of *IL-6* measured by ELISA and glucose concentration by glucose tolerance test (GTT) analysis in blood serum was significantly increased (Figures 2H and 2I).

miR-200c participates in adipogenic differentiation of hBMSCs

Figure 3 summarizes the mutual influence between *miR-200c* and adipogenic differentiation in hBMSCs. After differentiation, lipids accumulated in adipogenic differentiated hBMSCs under Oil Red O staining (Figure 3A). The transcripts of adipogenic markers, including peroxisome proliferator-activated receptor γ (*PPAR-γ*) and lipoprotein lipase (*LPL*) in the hBMSCs, were significantly increased for cells cultured in the differentiation medium than those cultured in the control medium (Figures 3B and 3C). The transcripts of noggin and leptin increased in adipogenic differentiated cells. Interestingly, the adipogenic differentiation significantly downregulated *miR-200c* in hBMSCs. In addition, after a plasmid-based miRNA inhibitor system

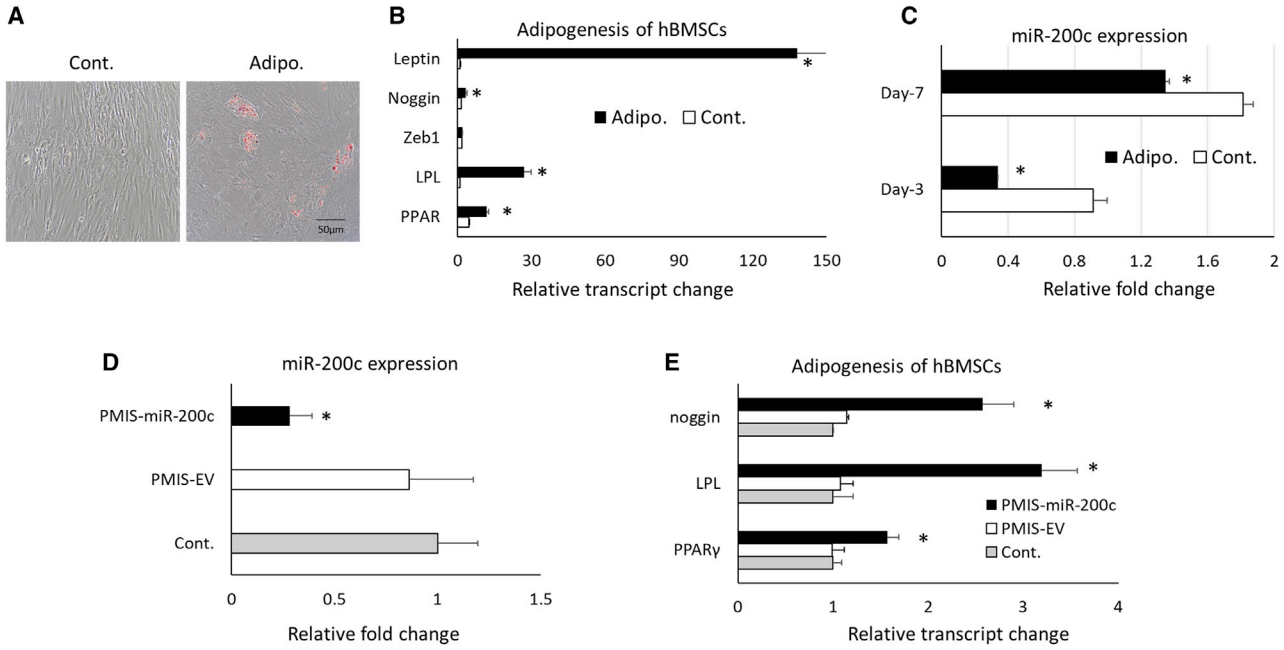

Figure 3. Characteristics of adipogenesis of hBMSCs on miR-200c expression

(A) Microphotographs of hBMSCs with Oil Red O staining 3 weeks after adipogenic differentiation and control. (B) Relative transcript changes of *noggin*, *Zeb1*, *LPL*, *PPAR-γ*, and *leptin* of hBMSCs 1 week after adipogenic differentiation compared to controls. (C) Relative fold change of *miR-200c* hBMSCs 3 and 7 days after differentiation and controls. (D) Normalized fold changes of *miR-200c* expression in hBMSCs 3 days after treatment with PMIS-miR-200c. (E) Relative transcript changes of *PPAR-γ*, *LPL*, and *noggin* in adipogenic differentiated hBMSCs pretreated with PMIS-*miR-200c*. *$p < 0.05$, performed in triplicate.

(PMIS) effectively downregulated endogenous *miR-200c* expression, the adipogenic markers, including *PPAR-γ*, *LPL*, and *noggin*, were significantly increased in hBMSCs (Figures 3D and 3E).

LPS-induced periodontal inflammation in DIO mice mimicked the pathophysiological variabilities of PiOSs

Figure 4 summarizes pathophysiological variabilities after injection of Pg-LPS into the gingival sulcus between maxillary M1/M2 of obese mice after 16 weeks of being fed an HFD. After 2 weeks, the injection of Pg-LPS induced apparent AB resorption compared to PBS as shown in micro-computed tomography (μCT) images (Figure 4A). Quantitatively, the distances between the Cementoenamel Junction (CEJ) to the AB crest (ABC) measured by μCT were significantly increased in mice with Pg-LPS injection over controls (Figure 4B). Pg-LPS injection also significantly reduced the parameter of AB microarchitecture in the maxilla, including the bone volume/tissue volume (BV/TV) and bone mineral density (BMD; Figures 4C and 4D). Pg-LPS also downregulated *miR-200c* in the gingiva (Figure 4E). Injection of Pg-LPS significantly increased transcripts of *IL-6* and *Zeb1* in gingiva and *IL-8* in WAT (Figures 4F and 4G). Although both *IL-8* in gingiva and *IL-6* and *Zeb1* in WAT were increased, no statistical difference was observed due to limited sample size. In addition, DIO mice injected with LPS have significantly increased glucose intolerance and insulin resistance than do control mice receiving PBS injection as evidenced by an increased glucose concentration through GTT analysis (Figure 4H).

Local injection of miR-200c at gingival tissues attenuated local and systemic inflammation in a mouse model of PiOSs

We injected naked plasmid DNA encoding *miR-200c* into gingival tissues of obese mice with periodontitis to test the protective function of *miR-200c*. Pg-LPS at 20 μg was injected into the interdental region between M2/M3 of DIO mice to create a mouse model of PiOSs. PBS was injected as a control. Plasmid DNA encoding *miR-200c* at 1 and 5 μg was applied to treat periodontitis, and plasmid encoding empty vector (EV) at 5 μg/μL was used as a treatment control. Mice were euthanized after 2 and 4 weeks, and periodontal and systemic inflammation and glucose metabolism were analyzed. Compared to the injection with PBS, in μCT images, injection of Pg-LPS co-treated with EV increased the distances between the CEJ to the ABC and induced AB resorption between M2 and M3 (Figure 5A). The histological examination after hematoylin and eosin (H&E) and tartrate-resistant acid phosphatase (TRAP) stains confirmed that the majority of AB between M2/M3 was resorbed after injection of Pg-LPS. Inflammatory granulation tissue and activated osteoclasts were observed in mice injected with Pg-LPS co-treated with EV (Figures 5B and 5C). However, in PiOS mice treated with *miR-200c*, limited bone resorption and inflammation induced by Pg-LPS were observed, and ABC was comparable to mice injected with PBS (Figures 5A–5C). Quantitatively, whereas Pg-LPS injection treated with EV resulted in significantly increased distance between the CEJ to the ABC, the treatment of *miR-200c* effectively restored the bone loss (Figure 6A). *miR-200c* also significantly restored BMD and BV/TV in the AB of maxilla after challenge with Pg-LPS

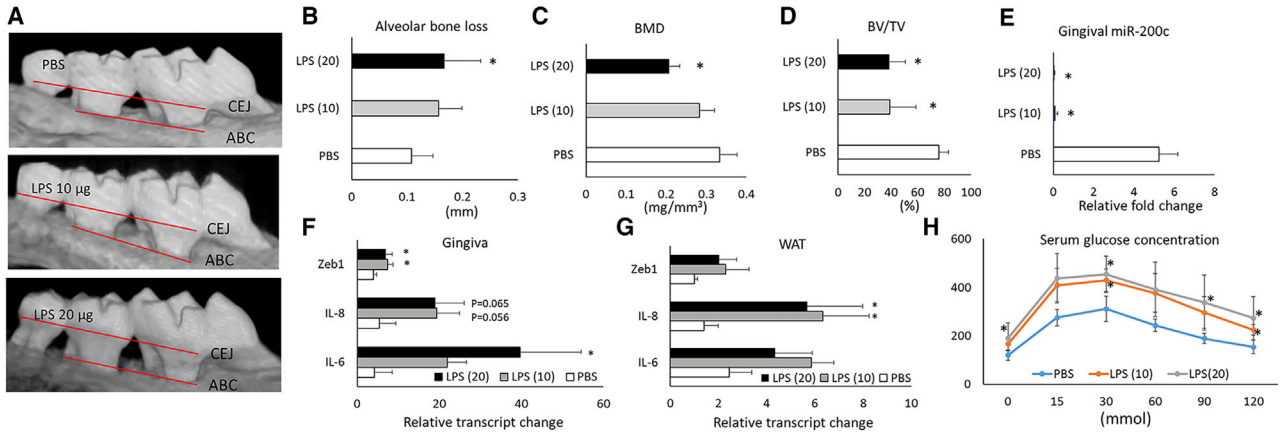

Figure 4. Pathophysiological characteristics of Pg-LPS injection into the gingival sulcus between maxillary M1/M2 of obese mice after 16 weeks of being fed an HFD

(A) μCT scan of maxillary bones on the palatal side of obese mice 2 weeks after receiving Pg-LPS at different concentrations. (B–D) Quantitative measurement of AB loss, BMD, and BV/TV at maxillary M1/M2 of mice. (E) Relative fold change of *miR-200c* in gingival tissues of mice with different treatments. (F and G) Relative transcript changes of IL-6, IL-8, and Zeb1 in gingiva and WAT of mice after different treatments. (H) Serum glucose concentration measured by a GTT test in mice with different treatment. *$p < 0.05$ versus PBS injection; n = 3–6.

(Figures 6B and 6C). Compared to the EV treatment, *miR-200c* injection also effectively rescued *miR-200c* downregulated by Pg-LPS after 2 weeks (Figure 6E). Treatment of *miR-200c* also significantly suppressed the *IL-6* transcript in the gingiva (Figure 6E). Notably, the injection of *miR-200c* at 5 μg significantly reduced the protein level of IL-6 in blood serum (Figure 6D) after 4 weeks. The local application of plasmid DNA encoding *miR-200c* also significantly increased the transcripts of *miR-200c* and reduced transcripts of *IL-6* and *IL-8* in WAT after 4 weeks (Figure 6F). In the GTT analysis, *miR-200c* treatment in gingival tissues reduced glucose concentration in PiOSs significantly.

Exosomal miR-200c probably mediated the anti-inflammatory function in treating PiOS mice

After plasmid *miR-200c* was injected into the gingival tissues of DIO mice, an increase of *miR-200c* expression in circulating exosomes was observed, compared to the injection of plasmid EV (Figure 7A, $p = 0.075$, n = 3; Figure 7A). In addition, we collected *miR-200c*-enriched exosomes from the supernatant of human embryonic palatal mesenchymal cells (HEPMs) with *miR-200c* overexpression. Transmission electron microscopy (TEM) and western blot were used to confirm the exosomes (Figure 7B). In order to determine the function of exosomal *miR-200c* on adipose tissue, human adipose derived stromal cells (hADSCs) were treated with the exosomes collected from the HEPM cells with *miR-200c* overexpression and the exosomes from the cells with EVs. The exosomes released from HEPM with *miR-200c* overexpression significantly increased *miR-200c* (~27-fold; Figure 7C) and reduced the transcripts of *IL-6* and *IL-8* in hADSCs. Exosomal *miR-200c* also significantly reduced *LPL* (Figure 7D).

Pg-LPS and IL-6 reduced miR-200c and increased Zeb1

Figure 8 summarizes the potential functions of *Pg-LPS* and *IL-6* on *miR-200c* and *Zeb1*. *IL-6* and Pg-LPS significantly downregulated *miR-200c* in a dose-dependent manner in HEPM. The anti-IL-6 mAb effectively rescued the reduction induced by Pg-LPS (Figures 8A and 8B). In addition, both *IL-6* and Pg-LPS upregulated *Zeb1*, while mAb against *IL-6* effectively counteracted the function of LPS on *Zeb1* (Figures 8C and 8D).

DISCUSSION

While different miRNAs and miRNA families have been reported to be predominantly expressed in certain tissues, the tissue-specific distribution of *miR-200c* remains unknown.[41] In this study, we compared *miR-200c* in different tissues of mice and found a significantly higher expression of *miR-200c* in gingival tissues than in blood, liver, and fat tissues. This finding suggested that *miR-200c* may have essential roles in the physiology and pathophysiology of oral gingival tissues. Because of the extensive regulation of *miR-200c* in inflammation and obesity,[32,33] this finding indicated that *miR-200c* may participate in the pathogenesis of periodontitis in obese patients.

Although many cytokines and miRs aggravate inflammation associated with periodontitis in obese subjects, the present study suggests that, for the first time, downregulation of *miR-200c* might play an important role in the molecular pathogenesis of PiOSs. While the variation of *miR-200c* in PiOSs in humans remains unknown, a significant downregulation of *miR-200c* was reported in gingival tissues of periodontitis patients.[29] Additionally, the finding that *miR-200c* is downregulated in blood samples of obese patients with insulin resistance also suggests that *miR-200c* may be downregulated in PiOS patients.[32] In this study, we have not only confirmed the previously published finding that *miR-200c* was downregulated in adipose tissue of obese mice,[33] but also found that obesity resulting from an HFD significantly reduced *miR-200c* in the gingival tissues. The DIO mice experienced increased IL-6 and impaired glucose tolerance,

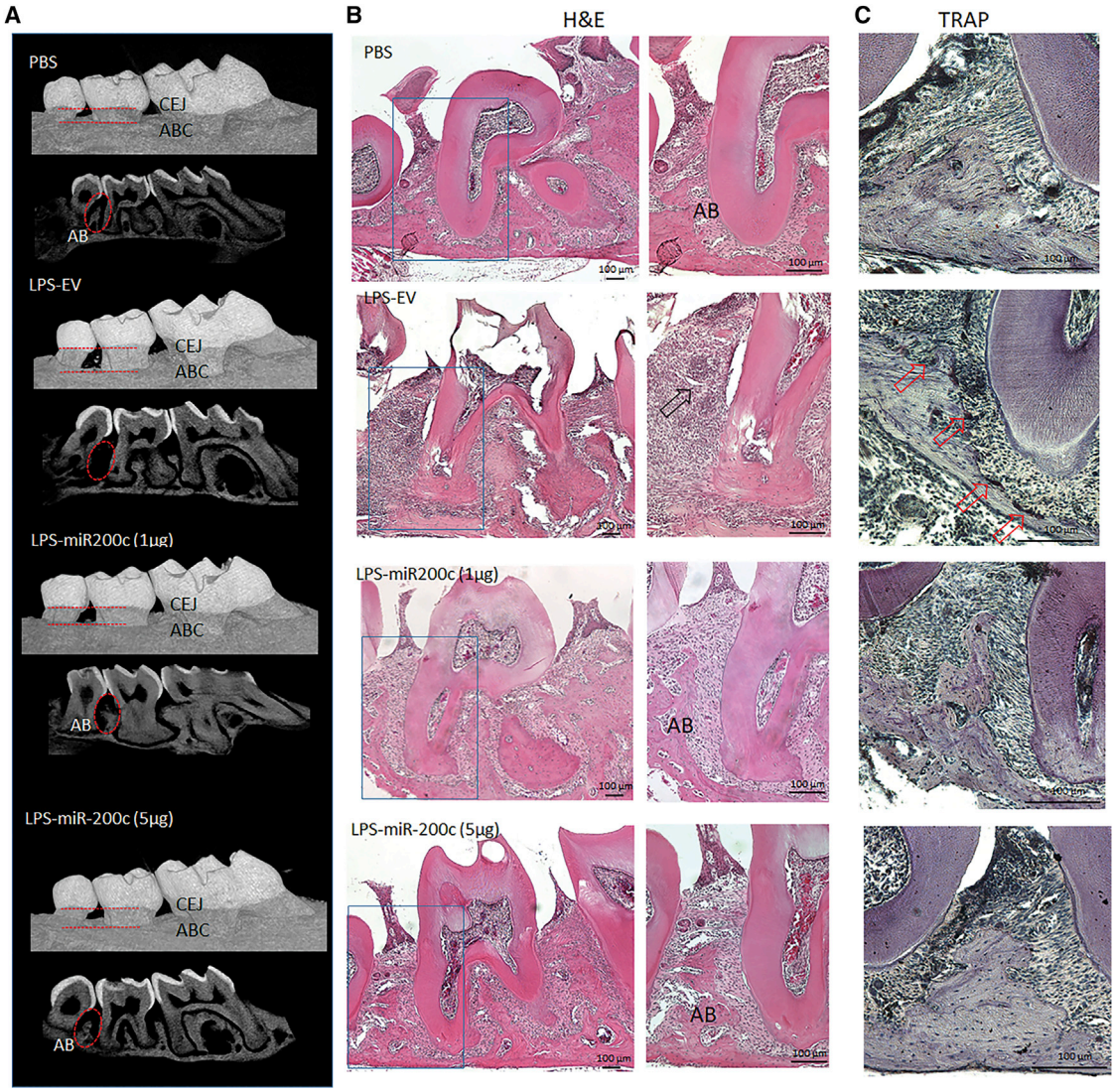

Figure 5. Representative μCT scan and microphotographs of histological cross-sections of obese mice 4 weeks after receiving Pg-LPS with *miR-200c* treatment and controls

(A) μCT images on the palatal side and cross-section of maxillary bones. (B) H&E-stained histological cross-section of mice after different treatments. AB, alveolar bone; arrow, granulation tissues; scale bar, 100 μm. (C) TRAP-stained histological cross-section of mice after different treatments. Arrow, activated osteoclasts; scale bar, 100 μm.

which are consistent with pathophysiological characteristics found in obese patients.[42,43] Administration of Pg-LPS in local gingival tissue not only caused AB loss and inflamed granulation tissues but also exaggerated the systemic inflammation evidenced by the upregulation of *IL-6* and *IL-8* and impaired glucose tolerance. These pathophysiological variations in obese mice with LPS injection were similar to variations for PiOS patients. *miR-200c* was significantly downregulated in gingival and adipose tissue in these mice. Thus, this strongly indicates that *miR-200c* most likely is downregulated in patient gingival tissues with PiOSs; however, human studies would be needed to confirm this. Additionally, because Pg-LPS represents the causal pathogen for chronic patient periodontitis, the similar pathophysiologies of PiOSs in this animal model allow us to further investigate its molecular pathogenesis and develop a treatment approach for PiOSs.

Our previous studies have reported the anti-inflammatory capabilities of *miR-200c* on periodontitis *in vitro* and *in vivo*. In this study, we have further confirmed that overexpression of *miR-200c* in gingival tissues, elicited by injecting naked plasmid DNA encoding *miR-200c*, could efficiently prevent periodontal inflammation and AB loss induced by LPS in obese mice. The local application of *miR-200c* also effectively protects the microarchitecture of AB. Moreover, we have demonstrated that the local application of *miR-200c* in gingival tissues could result in increased *miR-200c* in WAT. The latter

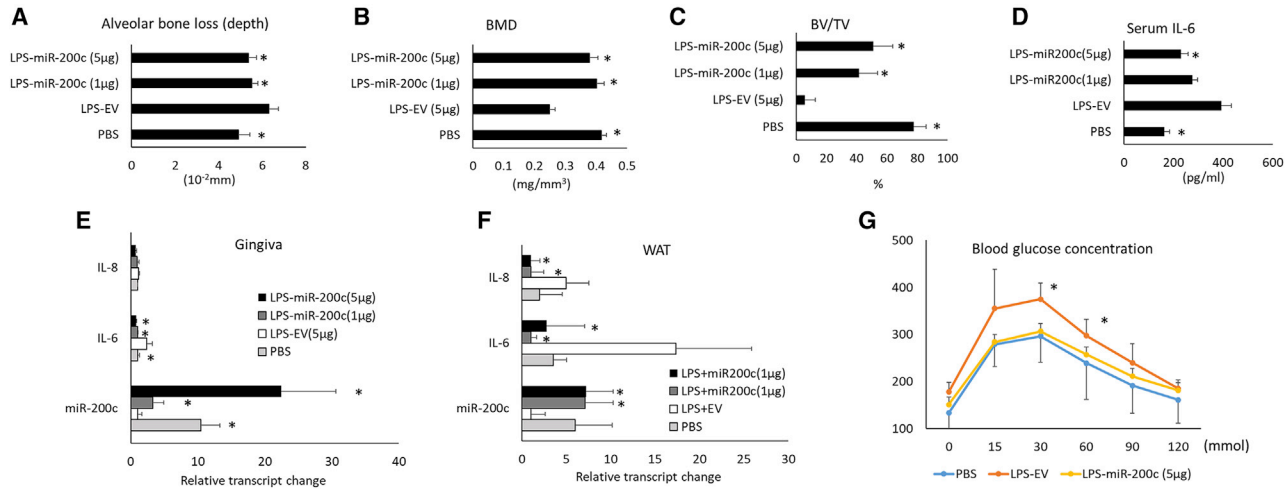

Figure 6. Quantitative measurements of the effectiveness of *miR-200c* on attenuating AB loss and systemic inflammation in obese mice with periodontitis

(A–C) Quantitative μCT measurement of AB loss (A), BMD (B), and BV/TV (C) at maxillary M2/M3 of obese mice with Pg-LPS injection 4 weeks after treatment with *miR-200c* at different concentrations and controls. (D) Serum concentration of IL-6 in mice 4 weeks after different treatments. (E and F) Relative transcript changes of *miR-200c*, *IL-6*, and *IL-8* in gingiva and WAT of mice with different treatments. (G) Serum glucose concentrations from a GTT test in mice 4 weeks after receiving different treatments. *$p < 0.05$ versus LPS-EV, n = 4–6.

potentially contributes to the downregulation of proinflammation cytokines, including transcripts of *IL-6* and *IL-8* in adipose tissues and IL-6 protein levels in blood. This indicates that local application of *miR-200c* in gingival tissue may also potentially improve the inflammatory status of obesity in PiOSs. In addition, we found that, for the first time, the local application of *miR-200c* effectively improved glucose tolerance and insulin resistance in obese mice with periodontitis. These results indicate a key potential benefit of local application of therapeutic *miR-200c* to alleviate both periodontitis and systemic glucose metabolism disorder associated with PiOSs. Although upregulated *miR-200c* found in type 2 diabetes was considered to increase apoptosis and impair pancreatic islets,[44] *miR-200c* was reported to be downregulated in blood samples from obese patients with insulin resistance, and the level of *miR-200c* is highly associated with whole body insulin sensitivity but inversely associated with insulin resistance and basal glucose. Opposite *miR-200c* expression levels may be caused by different pathophysiological variations in diabetes and obesity. In this study, we also observed that downregulation of *miR-200c* is associated with impaired glucose tolerance in DIO mice. The reduction of *miR-200c* and impaired glucose tolerance was even worse for DIO mice with LPS-induced periodontitis, which is similar to obese patients with periodontitis. Overexpression of *miR-200c* by injection of plasmid DNA into gingival tissues effectively improved glucose tolerance in PiOS mice. Although the underlying mechanism(s) is not clear, modulation of inflammation induced by overexpression of *miR-200c* may play a major role. We speculate that attenuated systemic inflammation with reduced circulating IL-6 levels and *IL-6* and *IL-8* transcripts in adipose tissues may contribute to this effectiveness. IL-6 has been demonstrated to decisively induce the development of insulin resistance and pathogenesis of type 2 diabetes mellitus through the generation of inflammation by controlling differentiation, migration, proliferation, and cell apoptosis.[45,46] Previous work has shown that IL-6 causes insulin resistance by impairing the phosphorylation of insulin receptor and insulin receptor substrate-1 by inducing the expression of SOCS-3, a potential inhibitor of insulin signaling.[47] Thus, downregulated *IL-6* in circulation and remote adipose tissue induced by overexpression of *miR-200c* in gingival tissues may play important roles in improving insulin resistance in PiOS mice.

In addition to the inhibitory function of obesity on *miR-200c*, we have also revealed the potential interactive regulation of *miR-200c* with adipogenesis in this study. First, we observed that the adipogenic differentiation of hBMSCs significantly downregulated *miR-200c*, which is consistent with downregulation of *miR-200c* in mice fed an HFD. We also noticed that downregulation of *miR-200c* could effectively promote adipogenic differentiation of hBMSCs, while overexpression of *miR-200c* could downregulate the adiopogenesis of hADSCs. There are several mechanism(s) probably involved in the regulation of *miR-200c*. *miR-200c* has been demonstrated previously to increase osteogenic differentiation.[39,48] Due to the inverse relationship between osteogenic and adipogenic programming, this may potentially explain the inhibitory role of *miR-200c* in adipogenesis. In addition, the reciprocal action between *miR-200c* and leptin, an adipokine activating proadipogenic factor,[49–51] may also explain aspects of regulation. Adipogenesis induced upregulation of leptin may potentially inhibit *miR-200c* while overexpression of *miR-200c* may act negatively on adipogenesis by suppressing noggin.[52,53]

In this study, we observed that circulating exosomal *miR-200c* in serum was upregulated after local injection of *miR-200c* in gingival tissues. Our *in vitro* test also demonstrated the anti-inflammatory

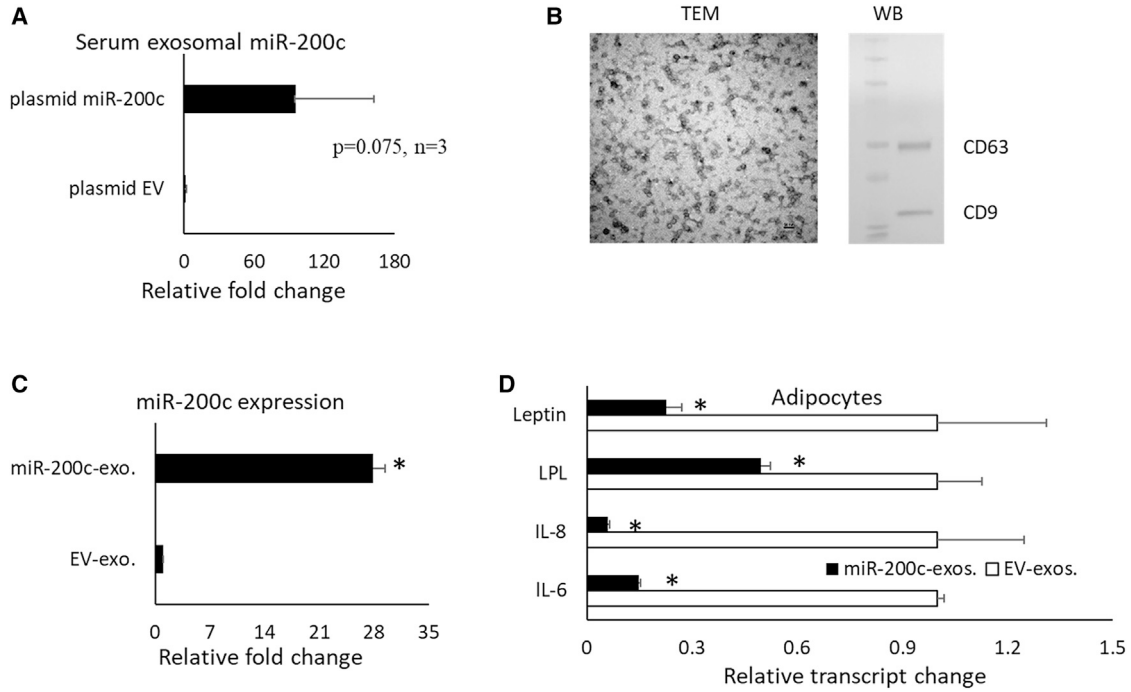

Figure 7. Exosomal *miR-200c* on inflammation and adipogenesis

(A) Relative fold change of *miR-200c* in serum exosomes isolated from mice receiving plasmid *miR-200c* injection in gingival tissues. p = 0.075, n = 3. (B) TEM image of exosomes isolated from HEPM cells with an overexpression of *miR-200c* and western blot using anti-CD63 and CD-9. (C) Relative fold changes of *miR-200c* in human ADSCs after treatment with exosomes isolated from HEPM cells with *miR-200c* overexpression and controls. (D) Relative transcript changes of *IL-6*, *IL-8*, and *LPL* in human ADSCs after treatment with exosomes isolated from HEPM cells with *miR-200c* overexpression and controls. *p < 0.05, performed in triplicate.

function of exosomal *miR-200c* using human adipose cells. Exosomes are known to be key mediators in cell-cell communication and facilitate the transfer of genetic and biochemical information between distant cells. Thus, we propose that circulating exosomes may transfer the genetic signals between gingival and adipose tissues and upregulation of circulating exosomal *miR-200c* may play a role in systemic anti-inflammation in PiOSs. However, future studies to confirm the origin of the circulating *miR-200c*-enriched exosomes and track their destinations in PiOSs will provide more information for determining the mechanism(s) mediating the interaction of gingival and adipose tissue in PiOSs.

Although IL-6 was reported to mediate *miR-200c* suppression in NF-κB signaling in a cancer study,[54] we reveal for the first time that IL-6 may directly inhibit *miR-200c* expression. That is, the downregulation of *miR-200c* in both mice and patients who are obese and have periodontitis is due to upregulated IL-6 levels. This finding provides further support for the role that *miR-200c* downregulation may play in PiOSs. In addition, previous studies have reported that Pg-LPS downregulates *miR-200c* in macrophages and gingival tissues potentially via regulation of *Zeb1*.[30,31] In this study, we not only confirmed the function of Pg-LPS on inhibiting *miR-200c* and increasing *Zeb1 in vitro* and *in vivo* but also observed the effectiveness of monoclonal antibodies in counteracting IL-6 *in vitro*. This strongly indicates that downregulation of *miR-200c* and upregulation of *Zeb1* induced by Pg-LPS may be mediated via the upregulation of *IL-6*. The upregulation of *Zeb1* further contributes to the downregulation of *miR-200c in vitro* and *in vivo*. However, the mechanism(s) underlying the inhibitory function of IL-6 on the biogenesis of *miR-200c* is not clear. In summary, the present studies have demonstrated that downregulation of *miR-200c* by upregulation of *IL-6*, *Zeb1*, and *leptin* in periodontitis and obesity may contribute to the molecular mechanism(s) of the pathogenesis of PiOSs by further exaggerating IL-6 levels and adipogenesis. Overexpression of *miR-200c* in gingival tissue can effectively attenuate both local and systemic inflammation and improve glucose metabolism in obese subjects by targeting *IL-6*, *IL-8*, *noggin*, and *leptin* (Figure 9). While the inhibitory function of IL-6 on *miR-200c* and circulating exosomal *miR-200c* may function in pathogenesis and treatment of PiOSs, respectively, future studies to confirm the function and clarify the underlying mechanism(s) are needed.

MATERIALS AND METHODS

Characterizing miR-200c and its potential regulators in DIO mice

All *in vivo* animal experiments were performed with approval from the Office of Animal Resources at the University of Iowa. The surgical protocols were followed in accordance with the policies and guidelines provided by the Institutional Animal Care and Use Committee. We first measured the tissue-specific distribution of *miR-200c*. Gingiva, liver, subcutaneous inguinal and epididymal WAT, and

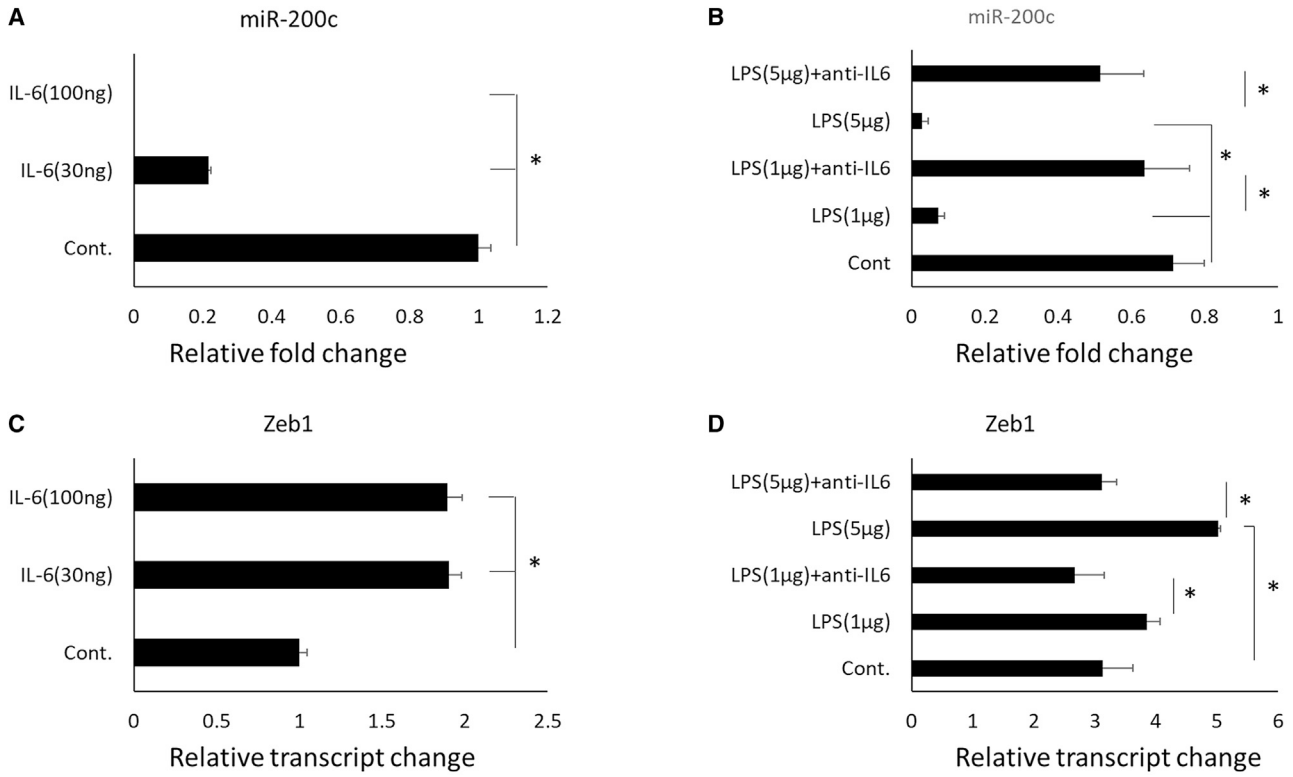

Figure 8. Effectiveness of IL-6 and LPS on *miR-200c* and *Zeb1*

(A and B) Relative fold changes of *miR-200c* expression in HEPM cells treated with IL-6 and LPS at different concentrations. (C and D) Relative transcript changes of *Zeb1* in HEPM cells treated with IL-6 and Pg-LPS at different concentrations. *$p < 0.05$, performed in triplicate.

blood serum were collected from 22-week-old male C57BL/6J mice (Jackson), and the transcripts of *miR-200c* were measured using qRT-PCR. In order to determine the influence of obesity on *miR-200c* and its regulators, we collected the gingiva and WAT from 12- and 22-week-old male C57BL/6J mice, respectively. The mice were fed with HFD (35.5% fat, 20% protein, and 32.7% carbohydrates) for 6 and 16 weeks. After each mouse was weighed and euthanized, the transcripts of *miR-200c*, *IL-6*, *IL-8*, *Zeb1*, and *noggin* were quantified using qRT-PCR. The protein level of *IL-6* in blood serum was measured using ELISA according to the manufacturer's protocol (BioLegend, San Diego, CA, USA). The GTT was performed to determine the glucose metabolism influenced by obesity. Mice of the same age on a RD were used as controls.

Evaluating miR-200c and its potential regulators in a mouse model of PiOSs

Periodontitis in obese mice was induced by Pg-LPS injection in male 22-week-old C57BL/6J mice fed with an HFD for 16 weeks. A total of 1 μL Pg-LPS (Biological Laboratories, Campbell, CA, USA) at 10 or 20 μg/μL was directly injected twice a week into the interdental region between maxillary molars using a Hamilton1700 series syringe. The same volume of PBS was injected into the same sites in controls. The mice were euthanized after 2 weeks, and the GTT test was performed before euthanization. The transcripts of *miR-200c*, *IL-6*, and *IL-8* in the gingiva, and WAT were measured using qRT-PCR, and the protein level of *IL-6* in blood was measured using ELISA. The AB resorption induced by Pg-LPS injection was analyzed using μCT.

Exploring the therapeutic effectiveness of miR-200c on PiOSs

To investigate the preventive and therapeutic potential of *miR-200c* for PiOSs, we injected Pg-LPS in gingival tissues of DIO mice to create a mouse model of PiOSs and co-treated with plasmid DNA encoding *miR-200c* at different doses or EV as a control. Plasmid DNA encoding *miR-200c* and EVs were prepared using methods described previously.[38,39] The mice were divided into four groups, each receiving a different treatment, including (1) PBS injection alone; (2) 20 μg of Pg-LPS with EV at 5 μg; (3) 20 μg of Pg-LPS injection with 1 μg of *miR-200c*; and (4) 20 μg of Pg-LPs injection with 5 μg of *miR-200c*. We injected 1 μL of the Pg-LPS with *miR-200c* or controls into the interdental region between M2/M3 twice a week. The mice were euthanized after 2 and 4 weeks, and the transcripts of *miR-200c*, *IL-6*, and *IL-8* from the gingiva, WAT, and protein levels of IL-6 in blood were measured using qRT-PCR and ELISA. GTT was performed to determine the influence of *miR-200c* on glucose metabolism in PiOSs after 4 weeks. The preventive function of *miR-200c* on AB resorption was measured using μCT and histology.

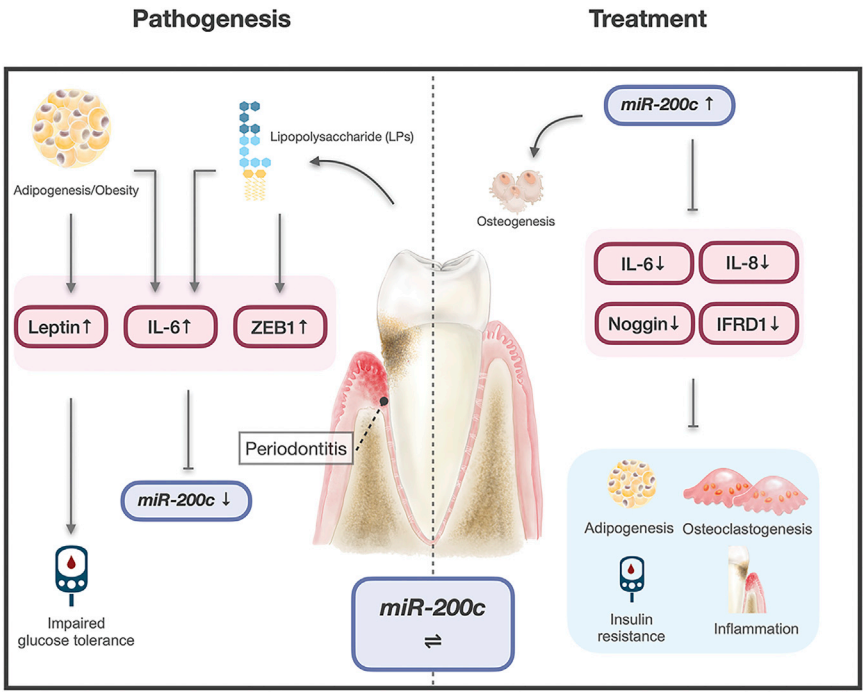

Figure 9. Potential roles of *miR-200c* in pathogenesis and treatment of PiOSs

Analyzing the influence of adipogenic differentiation on miR-200c *in vitro*

hBMSCs were purchased and cultured in complete mesenchymal stem cell growth medium (Lonza, Switzerland) at 37°C with 5% CO_2. At passage 4, the cells were seeded on a 12-well plate with a density of 10^5 cells/per well and cultured with adipogenic differentiation medium consisting of DMEM culture medium supplemented with 175 nM dexamethasone and 50 μM indomethacin for up to 21 days. Cells treated with DMEM culture medium containing 10% FBS and 1% antibiotics served as controls. The transcripts of *miR-200c* and adipogenic biomarkers, including *PPAR-γ* and *LPL*, were quantified using qRT-PCR after different time points. Oil Red O staining (Science) was performed to confirm the lipid accumulation after 21 days, as described previously.[55] In order to confirm the potential function of *miR-200c* on adipogenic differentiation, the adipogenic biomarkers in hBMSCs were measured after endogenous *miR-200c* was inhibited by a PMIS[56] (NaturemiRI, Iowa City, IA, USA).

Collecting and analyzing exosomal miR-200c in DIO mice and HEPM cells with miR-200c overexpression

A total of 1 μL of plasmid encoding DNA *miR-200c* at 5 μg/μL and PBS as a control was injected into gingival tissues at the labial vestibule of 22-week-old DIO mice twice a week. After 2 weeks, whole blood from the mice was collected from the venous sinus using a capillary tube and incubated at room temperature for 20 min. The serum was separated by centrifugation at 3,000 rpm for 15 min at 4°C and immediately aliquoted. Exosomes were subsequently extracted from serum using serum total exosome isolation kit (Invitrogen). The expression of *miR-200c* in serum and exosomes from the circulation of mice were measured using qRT-PCR. To determine the function of exosomal *miR-200c*, we collected *miR-200c*-rich exosomes from human embryonic palatal mesenchyme (HEPM) cells with overexpression of *miR-200c*. The HEPM cells with overexpression of *miR-200c* were prepared as previously described.[23] The *miR-200c*-enriched exosomes were collected from the supernatant of HEPM transduced with lentiviral *miR-200c* using exoEasy Maxi Kit (QIAGEN) according to the manufacturer's protocol. The exosome's characteristics, including spherical shapes with a size of 30–100 nm and CD63 and CD9, were confirmed using TEM and western blot. In order to determine the function of exosomal *miR-200c*, the *miR-200c* enriched exosomes were added to hADSCs (Lonza). ADSCs at passage 4 were seeded on a 12-well plate at 10^5 cells per/well and cultured in DMEM medium. A total of 20 μL exosomes at 3.7 μg/μL were added to hADSCs in an exosome-free medium for 18 h. The exosomes from the HEPM cells transduced with lentiviral EVs were used as controls. The transcripts of *miR-200c* and its targets, including *IL-6*, *IL-8*, and adipogenic marker in hADSCs, *LPL*, were quantified after 3 days using qRT-PCR.

Analyzing inhibitory roles of IL-6 on miR-200c

HEPM cells were cultured in DMEM medium and supplemented with *IL-6* at 30 and 100 ng/mL and LPS at 1 μg/mL. The range of *IL-6* concentrations was based on rates among patients with chronic periodontitis.[57] An anti-*IL-6* mAb was used to counteract the function of Pg-LPS. The transcripts of *miR-200c* and *Zeb1* were analyzed after 24 h using qRT-PCR.

qRT-PCR

Total RNA from mouse tissue and cultured cells was collected using miReasy mini kit (QIAGEN). The concentration and purity of the total RNA were quantified using a NanoDrop One Microvolume UV-Vis Spectrophotometer (Thermo Scientific). The measurement of *miR-200c* expression was performed using the mirScript ll reverse transcription kit and miRScript SYBR Green PCR Kit (QIAGEN) and normalized to *U6* by a comparative ΔΔCt method. mRNA expression was measured by qRT-PCR using PrimeScript Reagent Kit (Takara) to carry out reverse transcription and amplified reaction by using amplification primers with SYBR Green PCR Master Mix (PE Applied Biosystems). The comparative ΔΔCt method was used to quantify the relative level of different mRNA expression. All samples were normalized to GAPDH. Table 1 lists the primers for qRT-PCR.

Table 1. Sequence for forward and reverse primer sets used for real-time PCR

Gene	Forward primer (5′-3′)	Reverse primer (3′-5′)
PPAR-γ (H)	ACCAAAGTGCAATCAAAGTGGA	ATGAGGGAGTTGGAAGGCTCT
Noggin (H)	CCATGCCGAGCGAGATCAAA	TCGGAAATGATGGGGTACTGG
C/EBP-α (H)	TATAGGCTGGGCTTCCCCTT	AGCTTTCTGGTGTGACTCGG
ZEB1 (H)	GATGATGAATGCGAGTCAGATGC	ACAGCAGTGTCTTGTTGTTGT
IL-6 (H)	CCATCTTTGGAAGGTTCAGGTTG	ACTCACCTCTTCAGAACGAATTG
IL-8 (H)	AACCCTCTGCACCCAGTTTTC	ACTGAGGATTGAGAGTGGAC
LPL (H)	TGTGGTGGACTGGCTGTCA	CTGTCCCACCAGTTTGGTGTAG
GAPDH (H)	TGTGGGCATCAATGGATTTGG	ACACCATGTATTCCGGGTCAAT
IL-6 (M)	TAGTCCTTCCTACCCCAATTTCC	TTGGTCCTTAGCCACTCCTTC
IL-8 (M)	CAAGGCTGGTCCATGCTCC	TGCTATCACTTCCTTTCTGTTGC
Zeb1 (M)	CCATACGAATGCCCGAACT	ACAACGGCTTGCACCACA
Noggin (M)	GCGTCTCGTTCAGATCCTTCTC	GCCAGCACTATCTACACA

H, human; M, mouse

GTT measurement

For the GTT test, mice were food deprived for up to 16 h and subsequently administered up to 1 g/kg of glucose by intraperitoneal injection. Blood glucose was measured at t = 0, 15, 30, 60, 90, and 120 min, from 1–3 μL of blood obtained from a superficial nick made in the tail vein using a Breeze 2 glucose meter (Bayer).

μCT analysis

μCT analysis using SkyScan 1272 was performed to evaluate the AB resorption of mice with different treatments. Scanning was performed with a rotational angle of 360° around the longitudinal axis of the second molar tooth, utilizing a spatial resolution of 17 μm at 70 kV, 142 μA, and a 0.5° rotation step with an exposure time of 500 ms. Periodontal bone heights were measured as the distances from the CEJ to the ABC in the interdental region between M2 and M3. Volumetric measurements, including BV, TV, BV/TV, and BMD, were evaluated within the region of interest (ROI). The ROI of volumetric analysis of the interdental region was set between maxillary M2 and M3. The ROIs were drawn (size 0.19 × 0.414 = Ellipse) between the interproximal area of M2-M3 without overlap with the tooth. For image reconstruction, 2D virtual sections of maxillary molar teeth were acquired in the coronal, axial, and sagittal planes by the Skyscan CT-analyzer (CTAn) software. The CTAn software was further employed for 3D analysis and quantification of the volume of interfacial gaps and voids within the ROI. The Skyscan CT-Volume software was used for 3D visualization of periodontal bone tissues.

Histological examination

Maxillary tissue blocks in each group were fixated with 4% paraformaldehyde for 24 h at 4°C and decalcified with 10% ethylenediaminetetraacetate (EDTA) for 3 weeks. Subsequently, the samples were dehydrated in a gradient of ethanol before immersion 2 times in xylene. All samples were embedded in paraffin before sectioning. Sagittal sections of 8 μm thickness were cut perpendicular to the tooth axis. Sections were stained with H&E and TRAP staining following standard protocols. Corresponding images of the H&E- and TRAP-stained tissues were taken using a microscope to examine the AB loss.

Statistical Analysis

Descriptive statistics were conducted for both *in vitro* and *in vivo* investigations. For the *in vivo* study, a Student's t test was utilized to evaluate differences between DIO mice and controls at different time points. A one-way ANOVA with post hoc Tukey's HSD test was utilized to evaluate whether there was a significant difference in each measurement among mice with different treatments. The Shapiro-Wilks' test was also applied to verify the assumption of normality. All statistical tests completed for the *in vivo* quantification used a significance level of 0.05, and statistical analyses were performed using the statistical package SAS System version 9.4 (SAS Institute, Cary, NC, USA). For the *in vitro* study, a Student's t test was utilized to evaluate differences between the cells with adipogenic differentiation and controls. A one-way ANOVA with post hoc Tukey's HSD test was utilized to evaluate whether there was a significant difference in each measurement among cells with different treatments. The Shapiro-Wilks' test was applied to verify the assumption of normality. All statistical tests for the *in vitro* study utilized a significance level of 0.05, and statistical analyses were performed using commercially available SPSS 25 Statistical Software (IBM).

ACKNOWLEDGMENTS

The authors thank Dr. J. Michael Tilley and Professor Jeff Banas for proofreading and editing the manuscript. This study was supported by the National Institute of Dental and Craniofacial Research (grant nos. R21 DE024799 and R01 DE026433) of the National Institutes of Health (NIH).

AUTHOR CONTRIBUTIONS

Investigation, T.K., M.Z., Z.Z., S.E., Y.S., A.A., D.S.; writing – original draft preparation, T.K.; supervision, T.K., B.A.A., L.Y., L.H.; Q.Q.; formal analysis, F.Q.; conceptualization, B.A.A.; methodology, L.H.;

writing – review & editing, L.H.; funding acquisition, L.H.; visualization, L.H.

DECLARATION OF INTERESTS

L.H. and B.A.A. have a US patent for miR-200c-based bone regeneration. B.A.A. is the founder of the NaturemiRI Company.

REFERENCES

1. Chapple, I.L., Bouchard, P., Cagetti, M.G., Campus, G., Carra, M.C., Cocco, F., Nibali, L., Hujoel, P., Laine, M.L., Lingstrom, P., et al. (2017). Interaction of lifestyle, behaviour or systemic diseases with dental caries and periodontal diseases: consensus report of group 2 of the joint EFP/ORCA workshop on the boundaries between caries and periodontal diseases. J. Clin. Periodontol. *44* (*Suppl 18*), S39–S51.
2. Iwasaki, M., Kimura, Y., Ogawa, H., Yamaga, T., Ansai, T., Wada, T., Sakamoto, R., Ishimoto, Y., Fujisawa, M., Okumiya, K., et al. (2019). Periodontitis, periodontal inflammation, and mild cognitive impairment: A 5-year cohort study. J. Periodontal Res. *54*, 233–240.
3. Akram, Z., Abduljabbar, T., Abu Hassan, M.I., Javed, F., and Vohra, F. (2016). Cytokine Profile in Chronic Periodontitis Patients with and without Obesity: A Systematic Review and Meta-Analysis. Dis. Markers *2016*, 4801418.
4. Al-Rawi, N.H., and Shahid, A.M. (2017). Oxidative stress, antioxidants, and lipid profile in the serum and saliva of individuals with coronary heart disease: is there a link with periodontal health? Minerva Stomatol. *66*, 212–225.
5. Benguigui, C., Bongard, V., Ruidavets, J.B., Sixou, M., Chamontin, B., Ferrières, J., and Amar, J. (2012). Evaluation of oral health related to body mass index. Oral Dis. *18*, 748–755.
6. Hajishengallis, G. (2015). Periodontitis: from microbial immune subversion to systemic inflammation. Nat. Rev. Immunol. *15*, 30–44.
7. Pires, J.R., Dos Santos, I.P., de Camargo, L.F., Zuza, E.P., de Toledo, B.E., and Monteiro, S.C. (2014). Framingham cardiovascular risk in patients with obesity and periodontitis. J. Indian Soc. Periodontol. *18*, 14–18.
8. D'Aiuto, F., Sabbah, W., Netuveli, G., Donos, N., Hingorani, A.D., Deanfield, J., and Tsakos, G. (2008). Association of the metabolic syndrome with severe periodontitis in a large U.S. population-based survey. J. Clin. Endocrinol. Metab. *93*, 3989–3994.
9. Pischon, N., Heng, N., Bernimoulin, J.P., Kleber, B.M., Willich, S.N., and Pischon, T. (2007). Obesity, inflammation, and periodontal disease. J. Dent. Res. *86*, 400–409.
10. Chaffee, B.W., and Weston, S.J. (2010). Association between chronic periodontal disease and obesity: a systematic review and meta-analysis. J. Periodontol. *81*, 1708–1724.
11. Mathur, L.K., Manohar, B., Shankarapillai, R., and Pandya, D. (2011). Obesity and periodontitis: A clinical study. J. Indian Soc. Periodontol. *15*, 240–244.
12. Falagas, M.E., and Kompoti, M. (2006). Obesity and infection. Lancet Infect. Dis. *6*, 438–446.
13. Boesing, F., Patiño, J.S., da Silva, V.R., and Moreira, E.A. (2009). The interface between obesity and periodontitis with emphasis on oxidative stress and inflammatory response. Obes. Rev. *10*, 290–297.
14. Genco, R.J., Grossi, S.G., Ho, A., Nishimura, F., and Murayama, Y. (2005). A proposed model linking inflammation to obesity, diabetes, and periodontal infections. J. Periodontol. *76* (11, Suppl), 2075–2084.
15. Akram, Z., Safii, S.H., Vaithilingam, R.D., Baharuddin, N.A., Javed, F., and Vohra, F. (2016). Efficacy of non-surgical periodontal therapy in the management of chronic periodontitis among obese and non-obese patients: a systematic review and meta-analysis. Clin. Oral Investig. *20*, 903–914.
16. Gerber, F.A., Sahrmann, P., Schmidlin, O.A., Heumann, C., Beer, J.H., and Schmidlin, P.R. (2016). Influence of obesity on the outcome of non-surgical periodontal therapy - a systematic review. BMC Oral Health *16*, 90.
17. Srivastava, M.C., Srivastava, R., Verma, P.K., and Gautam, A. (2019). Metabolic syndrome and periodontal disease: An overview for physicians. J. Family Med. Prim. Care *8*, 3492–3495.
18. Costa, F.O., Cota, L.O., Cortelli, J.R., Cortelli, S.C., Cyrino, R.M., Lages, E.J., and Oliveira, A.P. (2015). Surgical and Non-Surgical Procedures Associated with Recurrence of Periodontitis in Periodontal Maintenance Therapy: 5-Year Prospective Study. PLoS ONE *10*, e0140847.
19. Xie, Y.F., Shu, R., Jiang, S.Y., Liu, D.L., and Zhang, X.L. (2011). Comparison of microRNA profiles of human periodontal diseased and healthy gingival tissues. Int. J. Oral Sci. *3*, 125–134.
20. Saito, A., Horie, M., Ejiri, K., Aoki, A., Katagiri, S., Maekawa, S., Suzuki, S., Kong, S., Yamauchi, T., Yamaguchi, Y., et al. (2017). MicroRNA profiling in gingival crevicular fluid of periodontitis-a pilot study. FEBS Open Bio *7*, 981–994.
21. McGregor, R.A., and Choi, M.S. (2011). microRNAs in the regulation of adipogenesis and obesity. Curr. Mol. Med. *11*, 304–316.
22. Nahid, M.A., Rivera, M., Lucas, A., Chan, E.K., and Kesavalu, L. (2011). Polymicrobial infection with periodontal pathogens specifically enhances microRNA miR-146a in ApoE-/- mice during experimental periodontal disease. Infect. Immun. *79*, 1597–1605.
23. Hong, L., Sharp, T., Khorsand, B., Fischer, C., Eliason, S., Salem, A., Akkouch, A., Brogden, K., and Amendt, B.A. (2016). MicroRNA-200c Represses IL-6, IL-8, and CCL-5 Expression and Enhances Osteogenic Differentiation. PLoS ONE *11*, e0160915.
24. Du, A., Zhao, S., Wan, L., Liu, T., Peng, Z., Zhou, Z., Liao, Z., and Fang, H. (2016). MicroRNA expression profile of human periodontal ligament cells under the influence of Porphyromonas gingivalis LPS. J. Cell. Mol. Med. *20*, 1329–1338.
25. Yue, J., Wang, P., Hong, Q., Liao, Q., Yan, L., Xu, W., Chen, X., Zheng, Q., Zhang, L., and Huang, D. (2017). MicroRNA-335-5p Plays Dual Roles in Periapical Lesions by Complex Regulation Pathways. J. Endod. *43*, 1323–1328.
26. Hill, L., Browne, G., and Tulchinsky, E. (2013). ZEB/miR-200 feedback loop: at the crossroads of signal transduction in cancer. Int. J. Cancer *132*, 745–754.
27. Humphries, B., and Yang, C. (2015). The microRNA-200 family: small molecules with novel roles in cancer development, progression and therapy. Oncotarget *6*, 6472–6498.
28. Kumar, S., Nag, A., and Mandal, C.C. (2015). A Comprehensive Review on miR-200c, A Promising Cancer Biomarker with Therapeutic Potential. Curr. Drug Targets *16*, 1381–1403.
29. Stoecklin-Wasmer, C., Guarnieri, P., Celenti, R., Demmer, R.T., Kebschull, M., and Papapanou, P.N. (2012). MicroRNAs and their target genes in gingival tissues. J. Dent. Res. *91*, 934–940.
30. Naqvi, A.R., Zhong, S., Dang, H., Fordham, J.B., Nares, S., and Khan, A. (2016). Expression Profiling of LPS Responsive miRNA in Primary Human Macrophages. J. Microb. Biochem. Technol. *8*, 136–143.
31. Sztukowska, M.N., Ojo, A., Ahmed, S., Carenbauer, A.L., Wang, Q., Shumway, B., Jenkinson, H.F., Wang, H., Darling, D.S., and Lamont, R.J. (2016). Porphyromonas gingivalis initiates a mesenchymal-like transition through ZEB1 in gingival epithelial cells. Cell. Microbiol. *18*, 844–858.
32. Masotti, A., Baldassarre, A., Fabrizi, M., Olivero, G., Loreti, M.C., Giammaria, P., Veronelli, P., Graziani, M.P., and Manco, M. (2017). Oral glucose tolerance test unravels circulating miRNAs associated with insulin resistance in obese preschoolers. Pediatr. Obes. *12*, 229–238.
33. Chartoumpekis, D.V., Zaravinos, A., Ziros, P.G., Iskrenova, R.P., Psyrogiannis, A.I., Kyriazopoulou, V.E., and Habeos, I.G. (2012). Differential expression of microRNAs in adipose tissue after long-term high-fat diet-induced obesity in mice. PLoS ONE *7*, e34872.
34. Tang, X., Wu, F., Fan, J., Jin, Y., Wang, J., and Yang, G. (2018). Posttranscriptional Regulation of Interleukin-33 Expression by MicroRNA-200 in Bronchial Asthma. Mol. Ther. *26*, 1808–1817.
35. Cao, Y., Liu, Y., Ping, F., Yi, L., Zeng, Z., and Li, Y. (2018). miR-200b/c attenuates lipopolysaccharide-induced early pulmonary fibrosis by targeting ZEB1/2 via p38 MAPK and TGF-β/smad3 signaling pathways. Lab. Invest. *98*, 339–359.
36. Wendlandt, E.B., Graff, J.W., Gioannini, T.L., McCaffrey, A.P., and Wilson, M.E. (2012). The role of microRNAs miR-200b and miR-200c in TLR4 signaling and NF-κB activation. Innate Immun. *18*, 846–855.
37. Chuang, T.D., and Khorram, O. (2014). miR-200c regulates IL8 expression by targeting IKBKB: a potential mediator of inflammation in leiomyoma pathogenesis. PLoS ONE *9*, e95370.

38. Akkouch, A., Zhu, M., Romero-Bustillos, M., Eliason, S., Qian, F., Salem, A.K., Amendt, B.A., and Hong, L. (2019). MicroRNA-200c Attenuates Periodontitis by Modulating Proinflammatory and Osteoclastogenic Mediators. Stem Cells Dev. *28*, 1026–1036.

39. Akkouch, A., Eliason, S., Sweat, M.E., Romero-Bustillos, M., Zhu, M., Qian, F., Amendt, B.A., and Hong, L. (2019). Enhancement of MicroRNA-200c on Osteogenic Differentiation and Bone Regeneration by Targeting Sox2-Mediated Wnt Signaling and Klf4. Hum. Gene Ther. *30*, 1405–1418.

40. Cao, H., Jheon, A., Li, X., Sun, Z., Wang, J., Florez, S., Zhang, Z., McManus, M.T., Klein, O.D., and Amendt, B.A. (2013). The Pitx2:miR-200c/141:noggin pathway regulates Bmp signaling and ameloblast differentiation. Development *140*, 3348–3359.

41. Ludwig, N., Leidinger, P., Becker, K., Backes, C., Fehlmann, T., Pallasch, C., Rheinheimer, S., Meder, B., Stähler, C., Meese, E., and Keller, A. (2016). Distribution of miRNA expression across human tissues. Nucleic Acids Res. *44*, 3865–3877.

42. Choi, Y.H., McKeown, R.E., Mayer-Davis, E.J., Liese, A.D., Song, K.B., and Merchant, A.T. (2014). Serum C-reactive protein and immunoglobulin G antibodies to periodontal pathogens may be effect modifiers of periodontitis and hyperglycemia. J. Periodontol. *85*, 1172–1181.

43. Kumar, N., Bhardwaj, A., Negi, P.C., Jhingta, P.K., Sharma, D., and Bhardwaj, V.K. (2016). Association of chronic periodontitis with metabolic syndrome: A cross-sectional study. J. Indian Soc. Periodontol. *20*, 324–329.

44. Belgardt, B.F., Ahmed, K., Spranger, M., Latreille, M., Denzler, R., Kondratiuk, N., von Meyenn, F., Villena, F.N., Herrmanns, K., Bosco, D., et al. (2015). The microRNA-200 family regulates pancreatic beta cell survival in type 2 diabetes. Nat. Med. *21*, 619–627.

45. Rehman, K., Akash, M.S.H., Liaqat, A., Kamal, S., Qadir, M.I., and Rasul, A. (2017). Role of Interleukin-6 in Development of Insulin Resistance and Type 2 Diabetes Mellitus. Crit. Rev. Eukaryot. Gene Expr. *27*, 229–236.

46. Park, S.E., Park, C.Y., and Sweeney, G. (2015). Biomarkers of insulin sensitivity and insulin resistance: Past, present and future. Crit. Rev. Clin. Lab. Sci. *52*, 180–190.

47. Kim, J.H., Bachmann, R.A., and Chen, J. (2009). Interleukin-6 and insulin resistance. Vitam. Horm. *80*, 613–633.

48. Xia, P., Gu, R., Zhang, W., Shao, L., Li, F., Wu, C., and Sun, Y. (2019). MicroRNA-200c promotes osteogenic differentiation of human bone mesenchymal stem cells through activating the AKT/β-Catenin signaling pathway via downregulating Myd88. J. Cell. Physiol. *234*, 22675–22686.

49. Howe, E.N., Cochrane, D.R., Cittelly, D.M., and Richer, J.K. (2012). miR-200c targets a NF-κB up-regulated TrkB/NTF3 autocrine signaling loop to enhance anoikis sensitivity in triple negative breast cancer. PLoS ONE *7*, e49987.

50. Howe, E.N., Cochrane, D.R., and Richer, J.K. (2011). Targets of miR-200c mediate suppression of cell motility and anoikis resistance. Breast Cancer Res. *13*, R45.

51. Chang, C.C., Wu, M.J., Yang, J.Y., Camarillo, I.G., and Chang, C.J. (2015). Leptin-STAT3-G9a Signaling Promotes Obesity-Mediated Breast Cancer Progression. Cancer Res. *75*, 2375–2386.

52. Blázquez-Medela, A.M., Jumabay, M., Rajbhandari, P., Sallam, T., Guo, Y., Yao, J., Vergnes, L., Reue, K., Zhang, L., Yao, Y., et al. (2019). Noggin depletion in adipocytes promotes obesity in mice. Mol. Metab. *25*, 50–63.

53. Sawant, A., Chanda, D., Isayeva, T., Tsuladze, G., Garvey, W.T., and Ponnazhagan, S. (2012). Noggin is novel inducer of mesenchymal stem cell adipogenesis: implications for bone health and obesity. J. Biol. Chem. *287*, 12241–12249.

54. Rokavec, M., Wu, W., and Luo, J.L. (2012). IL6-mediated suppression of miR-200c directs constitutive activation of inflammatory signaling circuit driving transformation and tumorigenesis. Mol. Cell *45*, 777–789.

55. Hong, L., Peptan, I.A., Colpan, A., and Daw, J.L. (2006). Adipose tissue engineering by human adipose-derived stromal cells. Cells Tissues Organs *183*, 133–140.

56. Cao, H., Yu, W., Li, X., Wang, J., Gao, S., Holton, N.E., Eliason, S., Sharp, T., and Amendt, B.A. (2016). A new plasmid-based microRNA inhibitor system that inhibits microRNA families in transgenic mice and cells: a potential new therapeutic reagent. Gene Ther. *23*, 634.

57. Batool, H., Nadeem, A., Kashif, M., Shahzad, F., Tahir, R., and Afzal, N. (2018). Salivary Levels of IL-6 and IL-17 Could Be an Indicator of Disease Severity in Patients with Calculus Associated Chronic Periodontitis. BioMed Res. Int. *2018*, 8531961.